Progress Report (ONR Award No. N00014-14-1-0804)

Quantum Spin Gyroscope

August 2014-July 2015

Report Type: Annual Report
Primary Contact E-mail: pcappell@mit.edu
Primary Contact Phone Number: 6172538137
Organization / Institution name: Massachusetts Institute of Technology
Grant/Contract Title: Quantum Spin Gyroscope
Grant/Contract Number: N00014-14-1-0804
Principal Investigator Name: Paola Cappellaro
Program Manager: Richard Tommy Willis

Abstract

Gyroscopes find wide application in everyday life, from navigation to rotation sensors in hand-held devices and automobiles. In addition, they can be used as inertial sensors to guide unnamed vehicles and to integrate Global Positioning Devices. Despite several advantages, including ease of fabrication, that have allowed conventional micro electro-mechanical systems (MEMS) gyroscopes to gain ubiquitous usage, they suffer from drifts after a few minutes of operation, making them unattractive for the most advanced applications. Other systems have different limitations, in particular the required large volumes.

Our project aims at overcoming these drawbacks by developing a novel solid-state quantum spin gyroscope associated with the Nitrogen-Vacancy (NV) centers in diamond. The NV center has recently emerged as a powerful quantum system, combining the good coherence properties and control techniques of atomic systems with the small size and fabrication capabilities of solid-state devices. These characteristics contribute as well to make this system a sensitive and compact rotation sensor. We plan to achieve even better performances by focusing on a gyroscope based on the nuclear spin associated with the NV center, which presents superior coherence properties.

In this technical report we outline the activities and accomplishments of the first year of the project, during which we performed enabling research, including building a compact device for the optical excitation and fluorescence collection of the NV centers as well as their magnetic resonance driving and characterization of diamond samples with high defect densities and of the Hamiltonian of the electronic-nuclear spin system.

1 Objectives of the research

Gyroscopes find wide application in everyday life, from navigation to rotation sensors in hand-held devices and automobiles. In addition, they can be used as inertial sensors to guide unnamed vehicles and to integrate Global Positioning Devices. Conventional commercial gyroscopes are built using micro electro-mechanical systems (MEMS) technology that allows for high sensitivities in a micron-size footprint. Despite several advantages, including ease of fabrication, that have allowed MEMS gyroscopes to gain ubiquitous usage, they suffer from drifts after a few minutes of operation, making them unattractive for the most advanced applications. While other systems that can be used as gyroscopes (such as ring laser gyroscopes or atomic interferometers), are not affected by the same causes of drift, they have other limitations, in particular the required large volumes.

Our project aims at overcoming these drawbacks by developing a novel solid-state quantum spin gyroscope associated with the Nitrogen-Vacancy (NV) centers in diamond. The NV center has recently emerged as a powerful quantum system, combining the good coherence properties and control techniques of atomic systems with the small size and fabrication capabilities of solid-state devices. We plan to achieve even better performances by focusing on a gyroscope based on the nuclear spin associated with the NV center, which presents superior coherence properties.

In the first year of the project, we performed enabling research that establishes the basis for the quantum gyroscope:

- We built a compact device for the optical excitation and fluorescence collection of the NV centers.
- We designed and tested microwave circuits to deliver the resonant fields for the nuclear and electronic spins
- We characterized diamond samples with high defect densities
- We characterized the Hamiltonian of the NV-14N system with unprecedented accuracy
- We analyzed and demonstrated enhanced driving of the nuclear spin thanks to forbidden transitions of the electronic spin

In the following, we provide further details of our activities and achievements

2 Design and Fabrication of the Quantum Gyroscope Prototype

In this first year we designed and fabricated the basic components of the quantum gyroscope, including optical excitation, fluorescence collection and microwave driving.

2.1 Optical excitation & Light collection

For testing purposes, the first iteration of the quantum gyroscope will use an external optical circuit to deliver the laser light needed for initialization and readout. The basic setup is shown schematically in figure 1.

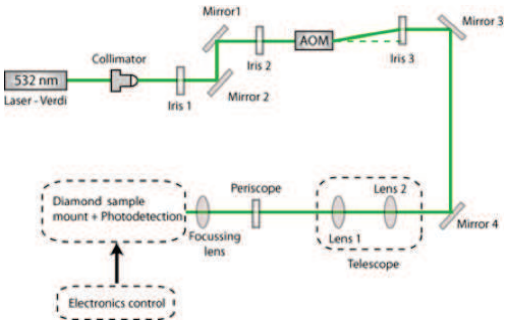

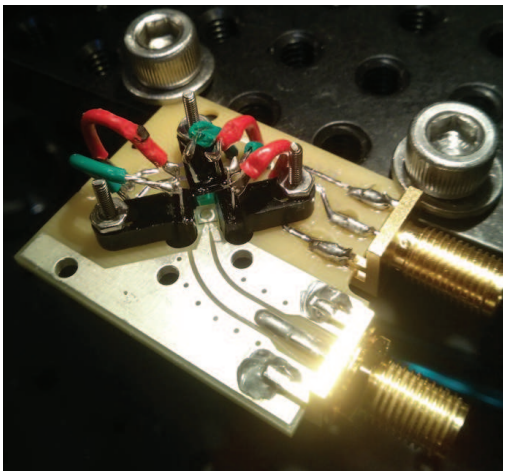

Fig. 1: Left: Schematics of the optical setup. Right: the light collection board, showing three photodetectors (black boxes) surrounding the diamond and connected with red/green cables to the PCB board.

The majority of the fluorescence emitted by NV centers is guided to the edges of the diamond chip via total internal reflection. Consequently, the fraction of the fluorescence signal detected can be greatly improved by placing photodetectors in contact with the diamond edges.

Using large active area photodiodes and a short stand-off distance between the sensor and the front of the photodiode packaging ensures that the photodiodes are able to collect the fluorescence signal within a wide solid angle. Filters with a pass band in the red wavelengths are used to cancel the excitation (green) light. The photodiodes are connected in parallel to traces on a printed circuit board (PCB) by short jumper wires. These traces are in turn soldered to an SMA connector that is connected to an external trans-impedance amplifier.

The experimental setup was first tested with a diamond sample presenting a very

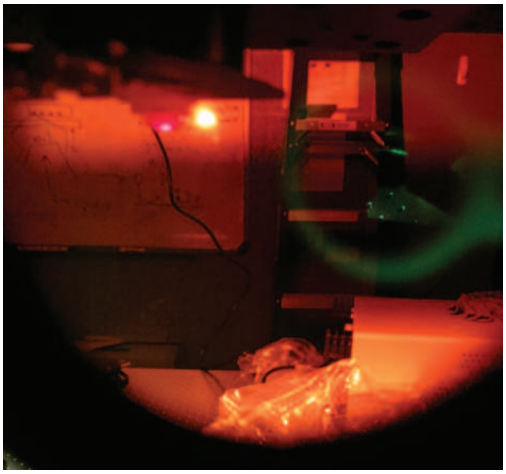

Fig. 2: The high density of defects in this diamond sample make it glow red. This picture was taken through a green-light filter while the sample is illuminated with just 20mW of green laser light.

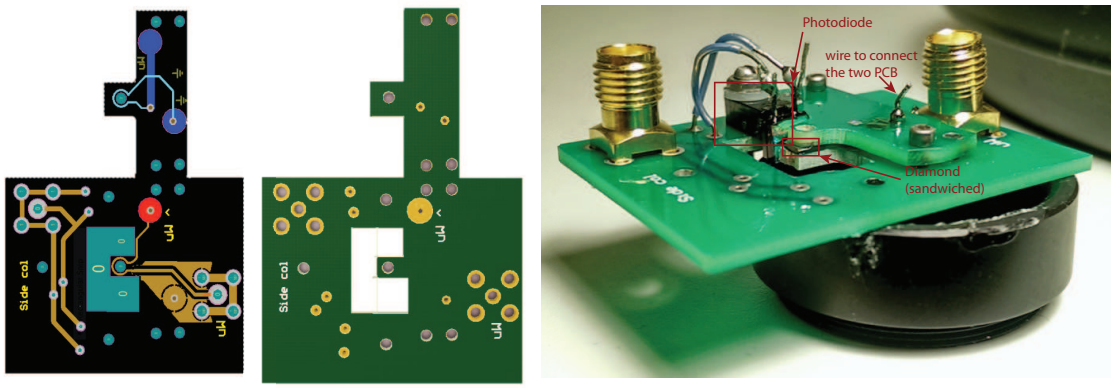

Fig. 3: Left: Design of the coplanar waveguide including circuitry for light collection. The thinner part on top is to be cut and superimposed to the larger part to deliver the microwave from two sides. Center: the fabricated PCB. Right: Mounted setup, including the diamond sample.

density of defects, $n_N = 2 \times 10^{19} cm^{-3}$. While this was a good sample in terms of optical properties, we found that the spin coherence properties were not good enough ($T_2 = 1\mu s$) due to the low conversion efficiency between nitrogen and NV.

2.2 Microwave Driving

Uniform driving of the electronic and nuclear spin is essential to the good performance of the quantum gyroscope. We thus designed and fabricated coplanar waveguides (CPW). A first, simple design provides a loop for the microwave driving, built together with the circuit needed for the light collection measurement. To improve on the vertical homogeneity, we designed a "sandwiched" structure, where microwaves are sent on both sides of the diamond.

We tested the CPW performing optically detected CW ESR and on-resonance Rabi nutation of the electronic spins (see figure 5). We observed increased homogeneity (as indicated by slower decay) thanks to the sandwich (Helmotz coil) configuration.

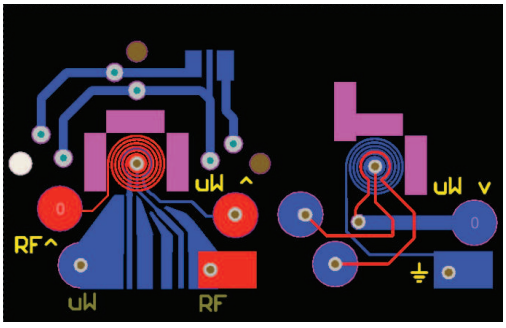

Fig. 4: CPW for RF driving

We have also designed a CPW capable of driving both the electronic and nuclear spin frequencies. Because of the weak coupling of the nuclear spins to external magnetic fields, it is necessary to drive strong currents through the rf coils. A strategy to increase the field created is to increase the number of loops of the coil. However, if the coils are small (and too close to each other) heating occurs, which affects the gyroscope performance. If instead the coils are too large (in order to ensure some minimum distance and coil thickness) the homogeneity of the field suffer. We thus optimized numerically the coil shape. We are currently testing the performance of our first generation of combined μw/rf coil.

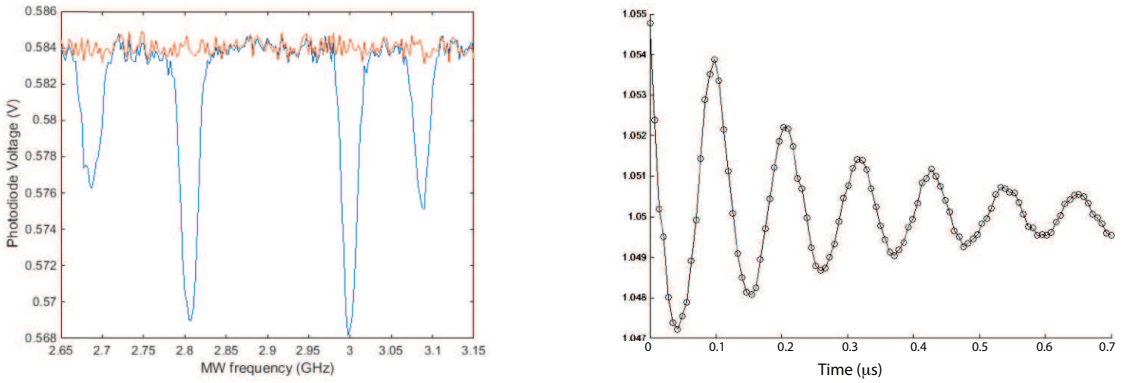

Fig. 5: Left: CW electronc spin resonance spectrum of the diamond sample, showing the characteristics peaks associated with the NV centers aligned along four different crystal axes. Here the magnetic field applied was $\sim$ 100G. Right: Rabi nutations

2.3 Sensitivity

In order to test the performance of this first, rough setup, we measured the magnetic field sensitivity. This can be easily translated into an expected, equivalent rotation sensitivity, as the proportionality factor is simply the electronic spin gyromagnetic ratio. More precisely, we studied the variation of the measured signal (fluorescence intensity) under a spin echo sequence when varying an external magnetic field. In addition, we measured the Allan deviation by increasing the number of averages, verifying that the measurement apparatus is indeed shot-noise limited. The magnetic field sensitivity is as low as $3\text{nT}/\sqrt{\text{Hz}}$. This corresponds to about $17\text{Hz}/\sqrt{\text{Hz}}$. Current limits to the sensitivity are due to residual inhomogeneities in the driving fields and, more fundamentally, the fact that until now we only used the electronic spin for sensing. The ultimate sensitivity and robustness of our quantum gyroscope scheme rests on the ability to use the nuclear spin associated with the NV center. While we are currently building the experimental capabilities to use the nuclear spins with the gyroscope ensemble setup, we have simultaneously built up better knowledge of the spin systems and of strategies for its control, as explained next.

3 Nuclear spin characterization and control

Precise knowledge of our quantum system's Hamiltonian is critical to develop the quantum gyroscope and more generally in any quantum technology such as quantum computation and sensing. In particular, the precise knowledge of the full hyperfine coupling tensor between the Nitrogen-Vacancy center (NV) electronic spin in diamond and the nitrogen nuclear spin enable its use as a rotation sensor and more broadly as an ancillary qubit resource in quantum algorithms and sensing protocols. However, measurement of the transverse part of the hyperfine coupling has not been performed to date with the accuracy afforded by working with single NV centers and needed for our gyroscope scheme. We thus performed the first precise measurement of the transverse hyperfine coupling using a single NV, harnessing enhanced forbidden transitions during resonant driving, which are strongly dependent on the hyperfine interaction.

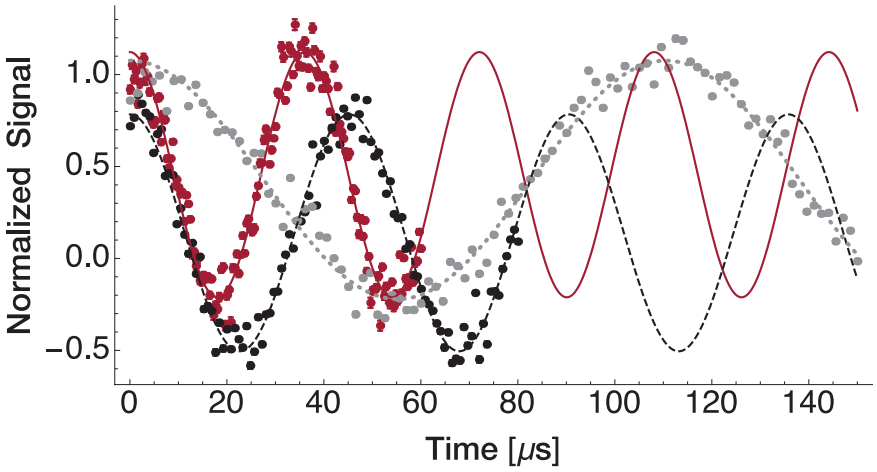

Fig. 6: ^{14}N Rabi oscillations at $B = 450$G, $B_1 \approx 3.3$G in the three NV manifold (Red, solid line $m_s = 0$. Black, dashed line, $m_s = -1$. Gray, dotted line $m_s = +1$). Here the dots are the experimental results, while the lines are fits to cosine oscillations. The different baseline of the $m_s = -1$ curve is due to small differences in the fluorescence emission of different nuclear manifolds.

The NV-14N spin system is characterized by the Hamiltonian

$$\mathcal{H} = \Delta S_z^2 + \gamma_e B_z S_z + (Q + \gamma_n B_z) I_z + A_\parallel S_z I_z + \sqrt{2} A_\perp (S_x I_x + S_y I_y). \quad (1)$$

Here S and I are the electron spin-1 and nuclear spin-1/2 operator respectively. $\Delta = 2.87$ GHz is the zero-field splitting and $Q = -4.945$ MHz the nuclear quadrupolar interaction. The NV spin is coupled to the nuclear spin by a hyperfine interaction with a longitudinal component $A_\parallel = -2.162$ MHz and a transverse component $A_\perp$ which we want to estimate. A magnetic field B_z is applied along the NV crystal axis [111] to lift the degeneracy of the $m_s = \pm 1$ level, yielding the electron and nuclear Zeeman frequencies $\gamma_e B_z$ and $\gamma_n B_z$ where $\gamma_e = 2.8$ MHz/G and $\gamma_n = -0.308$ kHz/G. While $A_\parallel$, the longitudinal (energy preserving) part of the hyperfine interaction with the NV electronic spin, has been accurately characterized, the transverse part $A_\perp$ had only previously been measured by ensemble ESR experiments. This interaction is difficult to be measured for single spins, since its signature is revealed in the NV electronic spin spectrum only for high and misaligned magnetic fields, which however kill the contrast between the spin states. We thus studied forbidden transitions in order to determine this parameter. This is further complicated by the fact that given the symmetry of the hyperfine tensors, the transverse terms only contribute under irradiation of the nuclear spin itself. The nuclear Rabi driving is enhanced with respect to what it would be in the absence of the electronic spin. The Rabi enhancement arises from hyperfine-mediated forbidden transitions. We can calculate the enhancement from a diagonalization of the internal Hamiltonian, which perturbs the driving

term. We obtain the enhancements:

$$\alpha_{+1} \approx 1 \quad + \quad \frac{\gamma_e}{\gamma_n} \frac{A_\perp}{\Delta + \gamma_e B_z - \gamma_n B_z - Q}, \tag{2}$$

$$\alpha_0 \approx 1 \quad - \quad \frac{\gamma_e}{\gamma_n} \Big(\frac{A_\perp}{\Delta + \gamma_e B_z - \gamma_n B_z - Q} + \frac{A_\perp}{\Delta - \gamma_e B_z - A_\parallel + \gamma_n B_z + Q} \Big), \tag{3}$$

$$\alpha_{-1} \approx 1 \quad + \quad \frac{\gamma_e}{\gamma_n} \frac{A_\perp}{\Delta - \gamma_e B_z - A_\parallel + \gamma_n B_z + Q}, \tag{4}$$

We note that while naively one would expect the maximum enhancement to be for $m_s = -1$ (where the difference in energy between the nuclear and electronic spin is minimum), because of constructive interferences to both ± 1 transitions from the 0 state, the enhancement in the $m_s = 0$ manifold can be larger.

Measuring the Rabi driving at different magnetic fields and in different manifolds we were able to determine the transverse hyperfine coupling B —as well as the longitudinal coupling A and the quadrupolar interaction Q, thus fully characterizing the nitrogen spin Hamiltonian.

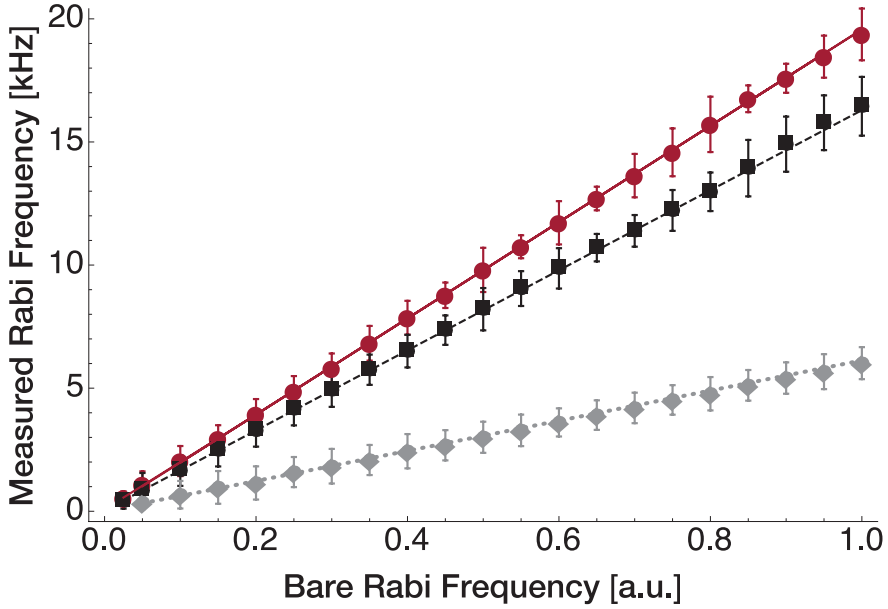

Fig. 7: Measured enhanced ^{14}N Rabi Frequency in the three NV manifold (Red, solid line $m_s = 0$. Black, dashed line, $m_s = -1$. Gray, dotted line $m_s = +1$) as a function of the bare Rabi frequency at $B = 509$G.

As changing the magnetic field is lengthy and complex, we fixed the magnetic field to 509G and instead linearly swept the amplitude of the RF driving (B_1). With this procedure, we do not need an independent measure of the bare Rabi frequency in order to extract the transverse hyperfine coupling strength. The relative RF amplitudes B_1 obtained when varying the driving strength can be measured at each nuclear resonance frequency by monitoring the RF voltage with an oscilloscope, confirming its linear dependence with applied power.

We thus measure the effective nuclear Rabi frequency as a function of the normalized RF amplitude

$B_1/|B_{1,max}|$ in all three electronic manifolds (Fig. 7). From the fit, we obtain an estimate of the transverse hyperfine coupling, $A_\perp = -2.62 \pm 0.05$ MHz, in good agreement with recently published values and with better precision than previously measured.

We also studied both theoretically and experimentally the enhancement of the nutation rate, which enables fast control of the nuclear spin even with moderate external driving and thus enable practical applications of the nuclear spin qubit. More generally, this novel method for measuring hyperfine coupling strengths can be applied to other electron-nuclear systems, such as phosphorus or antimony donors in silicon, defects in silicon carbide or quantum dots. Our result will thus have impact outside the current project and it will allow novel applications in quantum computing and metrology of the NV center, as the Nitrogen nuclear spin is emerging as an invaluable resource to implement more complex quantum algorithms and achieve improved sensitivity by e.g. repeated readouts or quantum error correction and feedback technique.

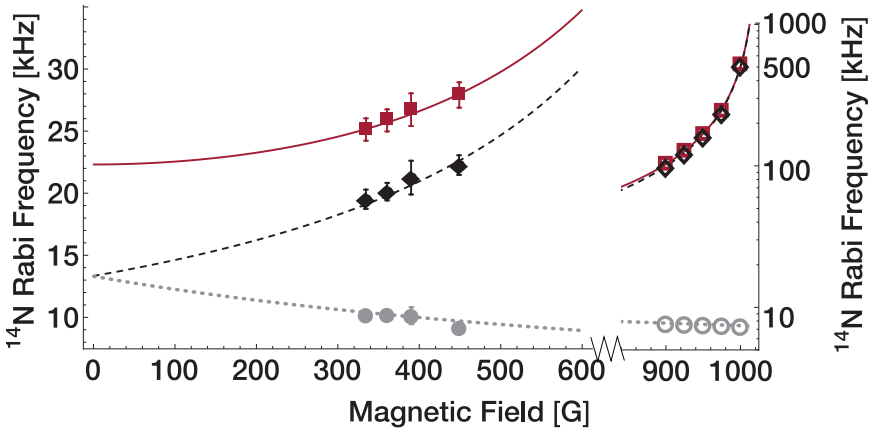

Fig. 8: ^{14}N Rabi Frequency in the three NV manifold (Red, solid line $m_s = 0$. Black, dashed line, $m_s = -1$. Gray, dotted line $m_s = +1$) as a function of the magnetic field. Rabi frequency corresponds to $\frac{\gamma_n B_1}{\sqrt{2}\pi}\alpha_{m_s}$. The filled symbols correspond to the experimental data, which matches closely the theoretical prediction. The effective Rabi frequencies increase rapidly with the field, exceeding 1 MHz when close to ground state level anti-crossing. The enhancement allows fast manipulation of the nuclear spin even when the bare Rabi field is only $B_1 \approx 3.3$G. The theoretical prediction is confirmed by simulations (open symbols) of the spin dynamics.

Presentations

- K. Saha, "Toward High-resolution sensing using color centers in diamond" *Rising Star Symposium, Massachusetts Institute of Technology*
- K. Saha, "High-resolution sensing with spin in diamond" *Indian Institute of Science*
- P. Cappellaro "Control of spin qubit registers in diamond" *SIPQNP (BBN, Cambridge, MA)*
- P. Cappellaro "Time-optimal control with a quantum actuator"" *INTRIQ (Institut Transdisciplinaire dInformation Quantique) Meeting, Chteau Bromont (Canada)*
- P. Cappellaro "Quantum Sensors" *NIST, Maryland*

Publications

[1] M. Chen, M. Hirose, and P. Cappellaro, "Measurement of transverse hyperfine interaction by forbidden transitions," *Phys. Rev. B*, vol. 92, p. 020101, Jul 2015.

[2] P. Cappellaro, "Polarizing nuclear spins in silicon carbide," *Physics*, no. 8, p. 56, 2015.

REPORT DOCUMENTATION PAGE

Form Approved
OMB No. 0704-0188

The public reporting burden for this collection of information is estimated to average 1 hour per response, including the time for reviewing instructions, searching existing data sources, gathering and maintaining the data needed, and completing and reviewing the collection of information. Send comments regarding this burden estimate or any other aspect of this collection of information, including suggestions for reducing the burden, to Department of Defense, Washington Headquarters Services, Directorate for Information Operations and Reports (0704-0188), 1215 Jefferson Davis Highway, Suite 1204, Arlington, VA 22202-4302. Respondents should be aware that notwithstanding any other provision of law, no person shall be subject to any penalty for failing to comply with a collection of information if it does not display a currently valid OMB control number.
PLEASE DO NOT RETURN YOUR FORM TO THE ABOVE ADDRESS.

1. REPORT DATE *(DD-MM-YYYY)*	2. REPORT TYPE	3. DATES COVERED *(From - To)*
07/15/2015	progress report	08/2014-07/2015

4. TITLE AND SUBTITLE
Quantum Spin Gyroscope

5a. CONTRACT NUMBER

5b. GRANT NUMBER
N00014-14-1-0804

5c. PROGRAM ELEMENT NUMBER

6. AUTHOR(S)
Paola Cappellaro

5d. PROJECT NUMBER
14PR11466-00

5e. TASK NUMBER

5f. WORK UNIT NUMBER

7. PERFORMING ORGANIZATION NAME(S) AND ADDRESS(ES)
MASSACHUSETTS INSTITUTE OF TECHNOLOGY
OFFICE OF SPONSORED PROGRAMS
RM E19 750 77 MASSACHUSETTS AVE
CAMBRIDGE, MA 02139-4301

8. PERFORMING ORGANIZATION REPORT NUMBER

9. SPONSORING/MONITORING AGENCY NAME(S) AND ADDRESS(ES)
Elizabeth Ford
Office of Naval Research
875 North Randolph Street
Arlington, VA 22203-1995

10. SPONSOR/MONITOR'S ACRONYM(S)
ONR

11. SPONSOR/MONITOR'S REPORT NUMBER(S)
ONR BD255

12. DISTRIBUTION/AVAILABILITY STATEMENT
Approved for Public Release; distribution is unlimited

13. SUPPLEMENTARY NOTES

14. ABSTRACT
Our project aims at overcoming drawbacks of current gyroscopes by developing a novel solid-state quantum spin gyroscope associated with the Nitrogen-Vacancy (NV) centers in diamond. In this technical report we outline the activities and accomplishments of the first year of the project, during which we performed enabling research, including building a compact device for the optical excitation and fluorescence collection of the NV centers as well as their magnetic resonance driving and characterization of diamond samples with high defect densities and of the Hamiltonian of the electronic-nuclear spin system.

15. SUBJECT TERMS

16. SECURITY CLASSIFICATION OF:			17. LIMITATION OF ABSTRACT	18. NUMBER OF PAGES	19a. NAME OF RESPONSIBLE PERSON
a. REPORT	b. ABSTRACT	c. THIS PAGE		10	Paola Cappellaro
					19b. TELEPHONE NUMBER *(Include area code)* 6172538137